Scientific Research Journal,
Vol 20, No 2 (2023) 115-129
https://doi.org/10.24191/srj.v20i2.22854

Investigation on the Effect of Bismuth Concentration Towards Radiation Shielding Properties in Ag-embedded Borobismuthate Mixed Ionic Electronic Glass System

Nurul Atika Mohd Khalid[1], Mazwani Mohd Rejab[1], Muhammad Naaim Mansor[1], Rosdiyana Hisam[1*]

[1]Faculty of Applied Sciences, Universiti Teknologi MARA, 40450 Shah Alam, Selangor, Malaysia

**Corresponding Author's E-mail: rosdiyana@uitm.edu.my*

Received: 26 June 2023
Accepted: 15 August 2023
Online First: 21 September 2023

ABSTRACT

In this study, $20Li_2O–xBi_2O_3–(79-x)B_2O_3–1Ag$ glasses for x=3,5,7,9, and 11 mol % glasses were prepared by using the melt quenching technique to investigate radiation shielding properties of the glasses using Phy-X/PSD simulation program at 15 keV to 15 MeV photon energy range. The radiation shielding parameters were carried out to determine the mass attenuation coefficient (MAC), linear attenuation coefficient (LAC), half value layer (HVL), mean free path (MFP) and effective atomic number (Z_{eff}). The results showed that the Bi_2O_3 addition has improved overall radiation shielding properties. The MAC of the glass system was increased as Bi_2O_3 concentration increased. The HVL showed that present glass better than standard commercial concretes as lower HVL value indicates better shielding where 11 mol % required a much smaller thickness than 3 mol %. Therefore, sample with highest bismuth content has the most effective radiation protective property. Smaller MFP is most preferable as it suitable for protection materials; indicated the 11 mol % is best candidate for radiation shielding. Lastly, the higher value in Z_{eff} was contributed by higher atomic number of Bi over B; thus, enhanced protection performance.

Keywords: Glass; Radiation Shielding; Borate; Silver Nano-Particles; Mixed Ionic Electronic

INTRODUCTION

Glass is an amorphous material made from inorganic substances at high temperatures, distinguishing it from other materials whose elements are heated to fusion and then cooled in a rigid state without crystallization. In radiation shielding applications, glasses are preferable to typical concrete or Pb-based materials due to their transparency to visible light. Various types of glass, such as borate, silicate, boro-silicate, phosphate, and tellurite-based glass, have been developed by scientists and researchers over several decades to generate high-quality radiation shielding glass [1].

Glass network formers are the oxides that form the backbone of the network. Borate is commonly employed as a glass former due to its chemical and thermal resistance, due to the interconnected BO_3 units. Borate can readily alter its oxidation state into BO_4 tetrahedral structures, which makes it an excellent host for metal ions. However, borate's low effective atomic number makes it unsuitable for use in shielding applications by itself [2]. Interestingly, the attenuation capabilities of glasses can be improved by doping them with heavy metal oxides (HMOs), or metal oxides with high densities [2]. Heavy metal-bismuth oxide (Bi_2O_3) can act as a glass intermediate which can switch role between glass modifiers or network which may increase stability, lower the temperature process, and inhibit moisture [3]. Previously, the addition of Bi_2O_3 in TeO_2-based glasses is significant because of their effectiveness in minimizing unwanted occupational and public radiation exposure in medical settings, as well as the clear view they provide when appropriately used during the using of diagnostic radiological facilities, mobile shields, and eye wears [4].

Besides that, the effect of alkali oxides and transition metal ions addition into glass former oxides such as tellurite, borate, and phosphate may induce mixed ionic electronic effect (MIE) which have been previously reported such as $10ZnO\text{-}xBi_2O_3\text{-}(90\text{-}x)B_2O_3$ [5], $(65\text{-}x)V_2O_5\text{-}xLi_2O\text{-}20TeO_2\text{-}15Bi_2O_3$ [6] and $Bi_2O_3\text{-}Fe_2O_3\text{-}P_2O_5$ [7]. Ionic conduction in glasses is contributed by monovalent alkali metal cations that travel through the oxygen-free sites of the glass network, whereas electronic conductivity is attributed to transition metal oxide via the polaron-hopping mechanism. Transition metal oxide can contribute to electrical conduction due to the features that allow it to exist in two oxidation states [8]. Previous study has found that mixed ionic-electronic glasses, such as Li_2O-V_2O_5-TeO_2 and Na_2O-V_2O_5-TeO_2 have conductivity minimums, which reflect linked behavior between ionic and electronic conductivity of the glasses [9].

Radiation shielding has been widely used in various fields such as medical diagnostic lab windows and doors, X-ray rooms and CT scans, scintillators, radiation therapy chambers, and space technology [10]. Transparent materials such as glass are significant as shielding materials, especially for radiotherapy room and imaging facilities [4]. Furthermore, bismuth-based glasses are used to replace lead-based glasses in the application of radiation shielding materials due to bismuth's larger atomic mass number, Z that associated with radiation attenuation and also less toxic [11]. In comparison to lead-silicate-based glass, adding Bi_2O_3 to silicate-based glass has resulted in greater density material with better shielding capabilities. In addition, a study that incorporates Bi_2O_3 in a zinc-borate glass system by Yasaka *et al.* [1] has showed that raising the quantity of bismuth oxide in the zinc-borate glass system can improve the mass attenuation coefficient. Moreover, the shielding properties of the transparent Bi_2O_3–B_2O_3–TeO_2 glass system have been compared to previously studied lead glass as a better shielding material option due to the lead-related problems such as high toxicity. On top of that, previous research reported that the presence of silver (Ag) nanoparticles in the glass matrix will enhance the radiation shielding ability of a material through better particle dispersion and larger surface area as it is expected that the incoming photon will be attenuated better due those reasons [12].

Nonetheless, the addition of electronic and ionic carriers in glass has resulted in an anomalous trend in other studied properties. Therefore, it is intriguing to evaluate the effect of MIE on the radiation shielding properties. In this current study, we attempted to study the effect of bismuth oxide increment on the radiation shielding of $20Li_2O$–xBi_2O_3–$(79\text{-}x)B_2O_3$–$1Ag$ glass for x = 3,5,7,9 and 11 mol %.

EXPERIMENTAL DETAILS

$20Li_2O–xBi_2O_3–(79-x)B_2O_3–1Ag$ mixed ionic electronic glass system for x = 3,5,7,9, and 11 mol % were prepared using the melt quenching method. High purity (>99%) raw materials were used such as lithium carbonate (Li_2CO_3), bismuth(III)oxide (Bi_2O_3), borone oxide (B_2O_3) silver (I) chloride (AgCl). The chemical powders were weighed accordingly using the analytical balance. Then, the mixtures were grinded for an hour using agate mortar and pestle to achieve homogenous. Then, the mixture was put in an alumina crucible hence melted in the electric furnace at a temperature of 1100 °C for an hour. The mixture was then quenched into a pre-heated stainless-steel mold hence annealed in at 350 °C for 2 h and eventually, cooled to room temperature.

Phy-X/PSD simulation program was used for calculating the important radiation shielding parameters accurately ranging from 0.015 to 15 MeV of photon energies [13]. Parameters such as mean free path (MFP), effective atomic number (Z_{eff}), half-value layer (HVL) and etc. are significant to define the glass's potential as radiation shielding materials.

RESULTS AND DISCUSSIONS

Mass attenuation coefficient (MAC)

The evaluation of the mass attenuation coefficients of glass with varying concentrations of Bi_2O_3 at various photon energies were calculated using the intensity of incident and transmitted (I) gamma rays at a given energy level abiding Beer-Lambert law as according to Equation (1) [14]:

$$I = I_0 exp^{\{-(\mu/\rho)t\}} \quad (1)$$

where I and I_0 are the transmitted and initial intensity of the radiation/ energy, respectively; t is the sample thickness and (μ/ρ) is the mass attenuation coefficient (MAC). Since MAC defines the ability for a material to attenuate radiation, a greater value denotes a more effective shield [2,15]. The MAC was used to describe penetration and interaction of photon with the materials and can be calculated using Equation (2) as follow[5]:

$$MAC = \mu_m = \frac{\mu}{\rho} = \sum_i W_i \left(\frac{\mu}{\rho}\right)_i \quad (2)$$

where (μ/ρ)i is the mass attenuation coefficient of its constituent element and wi is the weight fraction of its constituent elements in the glass sample.

The mass attenuation coefficient results for the $20Li_2O$-xBi_2O_3-(79-x) B_2O_3-1Ag glasses system, with increasing bismuth contents (x = 3,5,7,9 and 11 mol %) against photon energy were shown in Figure 1. In general, Figure 1 portrayed the MAC value of all glass samples decreased as photon energy increased and eventually, plateaued after 5 MeV. This is due to photoelectric absorption, Compton scattering, and pair formation processes that alters the MAC value within this energy range. As the intensity of the incoming radiation increases, more photons are able to travel through the sample, reducing its ability to absorb photons and declined the MAC values [2]. In addition, a peak emerged at around 0.1 MeV and referred as the Bi-absorption edge [16]. In respect to Bi_2O_3 content, glass with x =11 mol % has the highest value of MAC particularly at the lower energy region (E<0.1 MeV) and the MAC values decreased as Bi_2O_3 decreased where maximum values for all the glasses can be observed at the lowest tested energy (0.015 MeV) that equal to 21.383, 31.150, 39.192, 45.930 and 51.657 cm^2/g for x = 3, 5, 7, 9 and 11 mol % glasses, respectively. This is due to the dominant process of photoelectric effect that heavily relies on the atomic number of glass composition at lower region photon energy [17]. Therefore, it can be inferred that the glass samples are most effective at lower energies, with 11 mol % being the most effective, and as energy increases, their shielding ability becomes less effective. In short, x = 11 mol % glass sample has greater attenuation capabilities than the other investigated samples.

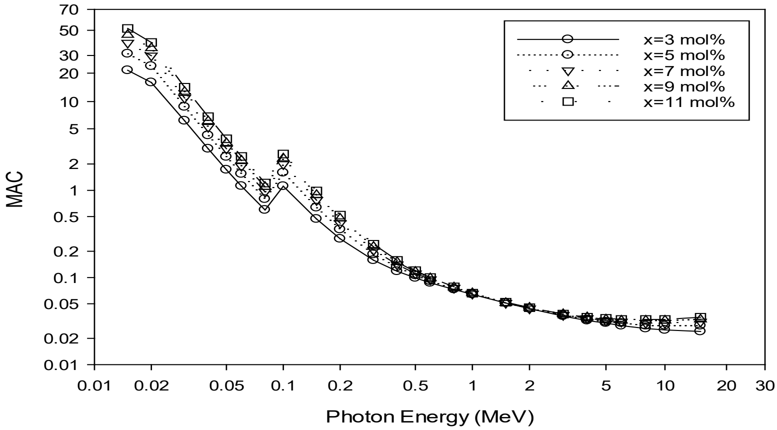

Figure 1: Plot of mass attenuation coefficients (MAC) against photon energy of $20Li_2O–xBi_2O_3$ (79-x)B_2O_3–1Ag glass system (x = 3,5,7,9 and 11 mol %)

Linear attenuation coefficient (LAC)

The plot of linear attenuation coefficient of $20Li_2O–xBi_2O_3$–(79-x) B_2O_3–1Ag (x = 3,5,7,9 and 11 mol %) glass samples against photon energy is shown in Figure 2. The LAC value is the multiplying product of the MAC values with the density of glass samples as shown in Equation (3):

$$(\mu/\rho) \times \rho = \mu \tag{3}$$

The graph in Figure 2 clearly indicated a reduction in the LAC values of glass samples against the incoming photon energy from 0.015−15 MeV which almost similar to the MAC (Figure 1). The LAC values for all the 5 different of Bi_2O_3 content dropped which were due to higher energy photons having greater penetrating power, reducing sample attenuation, and decreasing LAC. Peak at around 0.1 MeV can be attributed to Bi-absorption edge. The greatest values for the glasses are observed at the lowest tested energy which was at 0.015 MeV. In addition, the increment of Bi_2O_3 content in the glass has impacted the LAC value especially in the lower energy region (E<0.1 MeV) where the trend depicted is as follows: 11 mol% > 9 mol% > 7 mol% > 5 mol% > 3 mol%. For example, the LAC values at 0.02 MeV are 142.166 113.359, 90.083, 68.034 and 40.356 cm^{-1}, respectively. These results demonstrated a correlation between the LAC values and the density which caused the 11 mol% glass has the highest LAC coming from replacement of lighter borate with heavier bismuth oxide [18]. It can be concluded that the 11 mol % glass sample is the most desirable radiation shielding properties.

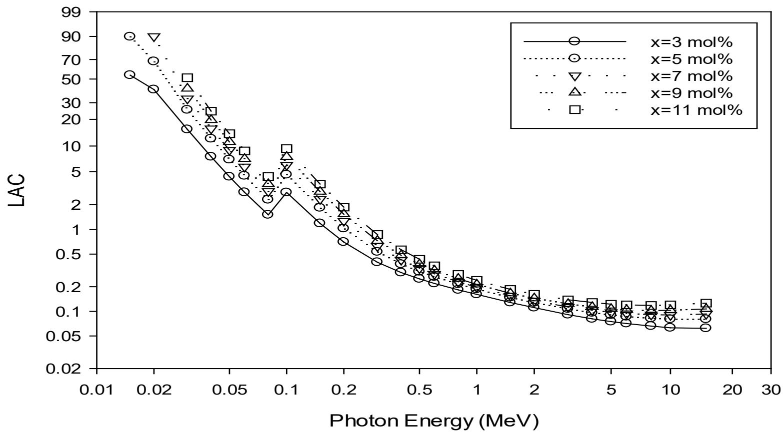

Figure 2: Plot of linear attenuation coefficients (LAC) against photon energy of $20Li_2O–xBi_2O_3–(79\text{-}x)B_2O_3–1Ag$ glass system (x = 3,5,7,9 and 11 mol %)

Half value layer (HVL)

The half value layer represents the material's thickness needed to cut the intensity of incoming radiation to half; hence a lower value of HVL indicated a better shield [2]. The HVL values for the glass in this study have been determined due to its significant in determining the radiation shielding ability of a material and can be evaluated via this relation shown in Eqaution (4) [19]:

$$HVL = \frac{0.693}{LAC} \tag{4}$$

Figure 3 depicted the plot of HVL values against photon energy of $20Li_2O–xBi_2O_3–(79\text{-}x)B_2O_3–1Ag$ glass system (x = 3,5,7,9 and 11 mol %). Based on the Figure 3, the HVL values obtained has increased against increasing photon energy and later, became constant at higher energy region (E>5 MeV) which reflect the declining effectiveness of the glass samples. In general, this indicates that a thicker glass is needed to half the intensity of higher-energy incoming photon to retain the glasses shielding efficiency. Moreover, Figure 3 also interpreted that the HVL values across samples have reduced over Bi_2O_3 addition owing to the increasing density of glass samples where glass sample with x = 3 mol % has the highest HVL values and the trend decreased with increasing Bi_2O_3 concentration, consecutively. These results signify that for the same photon energy, glass samples with x = 3 mol % of Bi_2O_3 content required a thicker glass than x = 11 mol % to reduce the intensity of the radiation to half of its original value. This stands that density influences the HVL reading of a material and lower HVL is to chase after which indicates better radiation shield. Therefore, higher density glass of x = 11 mol % has the most effective radiation protection property.

In addition, Table 1 has listed the HVL values for $20Li_2O–xBi_2O_3–(79-x)B_2O_3–1Ag$ (x = 11 mol %) glass sample where it is relatively lower than all the types of concretes at 0.6 MeV but slightly higher than some previous studied glass thus, it can be stated that the investigated glass is more effective, comparatively. In the light of this result, the $20Li_2O–xBi_2O_3–(79-x)B_2O_3–1Ag$ (x= 11 mol %) glass sample can be considered as an alternative for radiation shielding purposes in many areas especially application that needs better transparency.

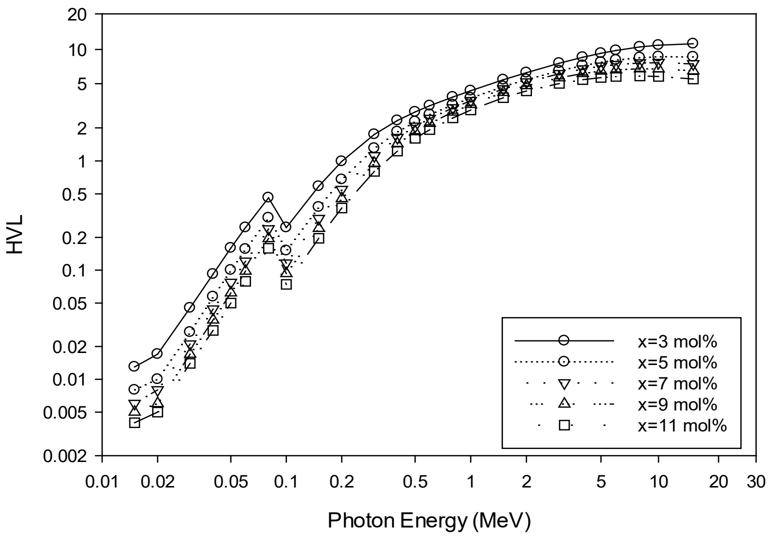

Figure 3: Plot of half value layer (HVL) against photon energy of $20Li_2O–xBi_2O_3–(79-x)B_2O_3–1Ag$ glass system (x = 3,5,7,9 and 11 mol %)

Table 1: The half value layer (HVL) values of some shielding concretes and commercial glasses at 0.6 MeV

Type of material	HVL (cm)
$20Li_2O–xBi_2O_3–(79\text{-}x)B_2O_3–1Ag$ (x = 11mol %)	1.927
Ordinary concrete [20]	3.867
Basalt-megnetite concrete [20]	2.899
Ilmenite concrete [21]	2.629
$xBi_2O_3 – (0.70 – x)B_2O_3–0.15SiO_2 – Na_2O$ (x=0.5 mol%) [21]	1.080
$xBi_2O_3 – (80 – x)B_2O_3 – 15SiO_2 – 5TeO_2$ (x=75 wt%) [21]	1.1929

Mean free path (MFP)

Mean free path is the average distance of a moving particle, such as photon that travels between successive collisions where smaller MFP indicates shorter distance traveled due to increase in the number of collisions between the incoming photon and the materials. Consequently, a smaller MFP is recommended. It can be determined by using Equation (5) [22]:

$$MFP = \frac{1}{\mu} \tag{5}$$

where μ is the linear attenuation coefficient (LAC). The MFP plot of $20Li_2O–xBi_2O_3–(79\text{-}x)B_2O_3–1Ag$ glass system (x = 3,5,7,9 and 11 mol %) against photon energy was plotted in Figure 4. The trend (Figure 4) depicted an increment as the photon energy increase and eventually, started to stagnate at higher energy region. It can be implied that as photon energy increases, the efficiency of the glasses decrease; hence, suggesting a denser material is needed to stop the higher energy phonon from penetrating deeper and worse, pass through the material. Based on the Figure 4, the MFP values were reduced as quantity of Bi_2O_3 content increased that contributes to higher density glasses owing to heavier bismuth weight and thus, increases the attenuation ability [18]. As such, the density of a material would affect the MFP value and therefore, influences the potential in shielding the incoming radiation where the denser glass sample (x =11 mol %) did best.

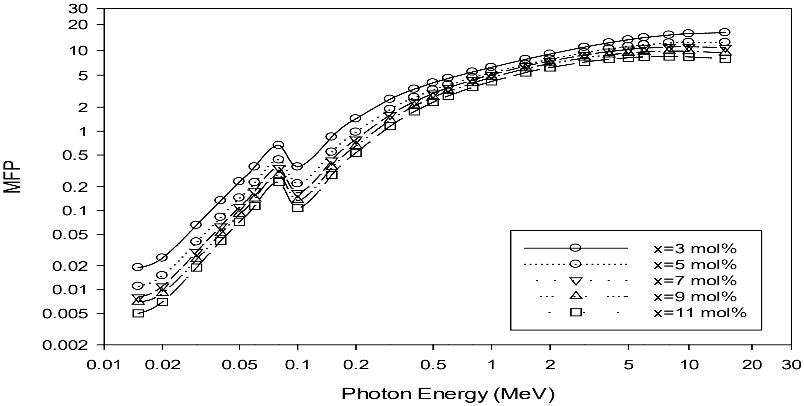

Figure 4: Plot of mean free path (MFP) against photon energy of $20Li_2O–xBi_2O_3–(79\text{-}x)B_2O_3–1Ag$ glass system (x = 3,5,7,9 and 11 mol %)

Effective atomic number (Z_{eff})

Effective atomic number values are frequently employed to explore the energy-dependent changes of materials obtained during the production of alternative radiation shielding materials. Z_{eff} is the average atomic number of a chemical with a higher value indicates a more effective shield [23]. In this study, Z_{eff} values were computed to determine the photon-material interactions and can be obtained through the total atomic cross section and total electronic cross section that related to Z_{eff} of the compound through Equation (6) [5]:

$$Z_{eff} = \frac{\sum f_i A_i (\frac{\mu}{\rho})_i}{\sum \frac{A_i}{Z_i} (\frac{\mu}{\rho})_j} \tag{6}$$

where f_i is the fractional abundance of the element i relative to the number of atoms providing that $\sum f_i = 1$, A_i is the atomic weight, and Z_i is the atomic number.

Figure 5 portrayed a generally decrease pattern of the Z_{eff} against increasing photon energy in $20Li_2O–xBi_2O_3–(79\text{-}x)B_2O_3–1Ag$ glass system (x = 3,5,7,9 and 11 mol %). Typically, materials with greater atomic number, Z will have greater Z_{eff} value. In Figure 5, the Z_{eff} values of the glass samples can be seen to rapidly decrease at lower photon energies

(E<0.1 MeV) as the photon energy increased. This is because of the change in dominant interaction process takes place from photoelectric effect that largely dependent on atomic number to Compton's scattering. Particularly, a sharp peak was observed at 0.1 MeV which due to K-absorption edge of Bi [16]. The trends continue to decrease until reached a minimum at 1 MeV before started to rise up again at 2 MeV which can be attributed to dominant interaction process change from Compton's scattering to pair production that slightly affected by the atomic number of the materials. Besides that, it can be seen that the glass samples with x = 11 mol % of Bi_2O_3 content has the highest Z_{eff} value followed by the others in descending manner of Bi_2O_3 content due to higher atomic number of Bi (Z=83) over B (Z=5) [16]. Therefore, it can be suggested that increasing Bi_2O_3 content in the glass system has improved the radiation shielding capability of the samples with respect to the Z_{eff} values.

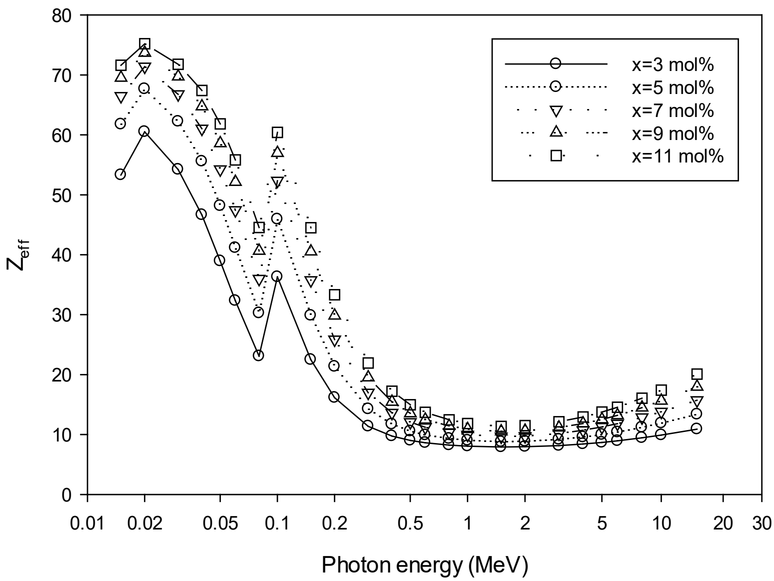

Figure 5: Plot of effective atomic number (Z_{eff}) against photon energy of $20Li_2O$–xBi_2O_3–$(79\text{-}x)B_2O_3$–1Ag glass system (x = 3,5,7,9 and 11 mol %)

CONCLUSION

Glass samples of $20Li_2O$-xBi_2O_3-$(79-x)Bi_2O_3$-1Ag for x = 3,5,7,9 and 11 mol % were successfully prepared using the melt quenching technique and hence, the radiation shielding properties of the glasses was investigated using Phy-X/PSD simulation program for energy range of 0.015−15 MeV. The glass with the 11 mol% of Bi_2O_3 content has the highest mass attenuation coefficient (MAC), shortest mean free path (MFP) and lowest half value layer (HVL) as compared with other glass samples due to higher density that coming from heavier bismuth weight compared with boron. Glass sample of 11 mol % Bi_2O_3 content has demonstrated better radiation shielding quality than some standard concretes based on HVL reading. The effective atomic number (Z_{eff}) results have increased over Bi_2O_3 concentration due to higher atomic number, Z of Bi (83) over B (5); hence, better protection performance. Therefore, it can be concluded that higher concentration of Bi_2O_3 was more suitable for radiation shielding purposes.

ACKNOWLEDGEMENT

The authors express gratitude to the Research Management Centre (RMC) and Universiti Teknologi MARA, Malaysia for assistance throughout the research. This study was financially supported by Universiti Teknologi MARA under the Geran Kolaborasi Entiti Penyelidikan UiTM (KEPU), 600-RMC/KEPU 5/3 (007/2023).

REFERENCES

[1] M. H. M. Zaid, H. A. A. Sidek, K. A. Matori, A. Abdu, K. A. Mahmoud, M. M. Al-Shammari, E. Lacomme, M. A. Imheidat, M. I. Sayyed, 2021. Influence of heavy metal oxides to the mechanical and radiation shielding properties of borate and silica glass system. *Journal of Materials Research and Technology*, 11, 1322-1330.

[2] E. Lacomme, M. I. Sayyed, H. A. A. Sidek, K. A. Matori, and M. H. H. Zaid, 2021. Effect of bismuth and lithium substitution on radiation shielding properties of zinc borate glass system using Phy-X/PSD

simulation. Results in Physics, 20, 103768.

[3] Q. Ma, X. Lv, Y. Wang, and J. Chen, 2016. Optical and photocatalytic properties of Mn doped flower-like ZnO hierarchical structures. *Optical Materials*, 60, 86-93.

[4] S. A. Tijani and Y. Al-Hadeethi, 2019. The influence of TeO_2 and Bi_2O_3 on the shielding ability of lead-free transparent bismuth tellurite glass at low gamma energy range. *Ceramics International,* 45(17), Part B, 23572-23577.

[5] D. Saritha, Y. Markandeya, M. Salagram, M. Vithal, A. K. Singh, and G. Bhikshamaiah, 2008. Effect of Bi_2O_3 on physical, optical and structural studies of $ZnO–Bi_2O_3–B_2O_3$ glasses. *Journal of Non-Crystalline Solids,* 354, 5573-5579.

[6] K. Keshavamurthy and B. Eraiah, 2016. Transport properties of lithium ions doped vanado-bismuth-tellurite glasses. *AIP Conference Proceedings*,1731,110002.

[7] A. Moguš-Milanković, A. Šantić, V. Ličina, and D. E. Day, 2005. Dielectric behavior and impedance spectroscopy of bismuth iron phosphate glasses. *Journal of non-crystalline solids,* 351, 3235-3245.

[8] M. S. Sutrisno, R. Hisam, and N. M. Samsudin, 2019. Anomalous behavior of optical properties in mixed ionic-electronic $20Li_2O-xBi_2O_3-(80-x)TeO_2$ doped silver nanoparticles tellurite glass system. *International Journal of Electroactive Materials,* 7, 53-66.

[9] J. E. Garbarczyk, M. Wasiucionek, P. Machowski, and W. Jakubowski, 1999. Transition from ionic to electronic conduction in silver–vanadate–phosphate glasses. *Solid State Ionics*, 119, 9-14.

[10] Y. S. Rammah, M. S. Al-Buriahi, and A. S. Abouhaswa, 2020. $B_2O_3–BaCO_3–Li_2O_3$ glass system doped with Co_3O_4: structure, optical, and radiation shielding properties. *Physica B: Condensed Matter*, 576, 411717.

[11] M. H. M. Zaid, K. A. Matori, H. A. A. Sidek, and I. R. Ibrahim, 2021. Bismuth modified gamma radiation shielding properties of titanium vanadium sodium tellurite glasses as a potent transparent radiation-resistant glass applications. *Nuclear Engineering and Technology,* 53, 1323-1330.

[12] M. S. Sutrisno, M. M. Naaim and R. Hisam, 2022. Effect of Ag nanoparticles addition on attenuation properties in 20Li_2O-5Bi_2O_3-(74-x)TeO_2-1Er_2O_3-xAg glasses. I*nternational Journal of Electroactive Materials*, 10, 52-56.

[13] E. Şakar, Ö. F. Özpolat, B. Alım, M. I. Sayyed, and M. Kurudirek 2020. Phy-X / PSD: Development of a user friendly online software for calculation of parameters relevant to radiation shielding and dosimetry. *Radiation Physics and Chemistry,*166,108496.

[14] Y. S. Alajerami, D. Drabold, M. H. A. Mhareb, K. L. A. Cimatu, G. Chen, and M. Kurudirek, 2020. Radiation shielding properties of bismuth borate glasses doped with different concentrations of cadmium oxides. *Ceramics International,* 46(8), Part B, 12718-12726.

[15] S. A. Shuhaimi, M. I. Sayyed, F. C. Hila, A. L. Anis, S. M. Iskandar, M. H. M. Zaid, M. N. Azlan, S. N. Nazrin, N. N. Yusof, R. Hisam, 2020. Effects of mixed TeO_2-B_2O_3 glass formers on optical and radiation shielding properties of 70[xTeO_2+(1−x)B_2O_3]+15Na_2O+15K_2O glass system. *Physica Scripta,* 97, 045804.

[16] M. I. Sayyed, I. A. El-Mesady, A. S. Abouhaswa, A. Askin, and Y. S. Rammah, 2019. Comprehensive study on the structural, optical, physical and gamma photon shielding features of B_2O_3-Bi_2O_3-PbO-TiO_2 glasses using WinXCOM and Geant4 code. *Journal of Molecular Structure,* 1197, 656-665.

[17] M. Kamislioglu, 2021. Research on the effects of bismuth borate glass system on nuclear radiation shielding parameters. *Results in Physics,* 22, 103844.

[18] N. Effendy, M. H. M. Zaid, H. A. A. Sidek, M. K. Halimah, M. K. Shabdin, K. A. Yusof, and M. Z. H. Mayzan, 2022. The elastic, mechanical and optical properties of bismuth modified borate glass: Experimental and artificial neural network simulation. *Optical Materials,* 126, 112170.

[19] S. J. Japari, M. I. Sayyed, A. K. Yahya, A. L. Anis, S. M. Iskandar, M. H. M. Zaid, M. N. Azlan, R. Hisam, 2021. Effects of Na_2O on optical and radiation shielding properties of xNa_2O-(20-x)K_2O-30V_2O_5-50TeO_2 mixed alkali glasses. *Results in Physics,* 22, 103946.

[20] A. Kumar, 2017. Gamma ray shielding properties of PbO-Li_2O-B_2O_3 glasses. *Radiation Physics and chemistry,* 136, 50-53.

[21] A. Saeed, R. M. El shazly, Y. H. Elbashar, A. M. Abou El-azm, M. M. El-Okr, M. N. H. Comsan, A. M. Osman, A. M. Abdal-monem, A. R. El-Sersy, 2014. Gamma ray attenuation in a developed borate glassy system. *Radiation Physics and Chemistry,* 102, 167-170.

[22] M. M. Naaim, M. F. Malek, M. I. Sayyed, N. F. M. Sahapini, and R. Hisam, 2022. Impact of TeO_2–B_2O_3 manipulation on physical, structural, optical and radiation shielding properties of Ho/Yb codoped mixed glass former borotellurite glass. *Ceramics International,* 49(7), 10342-10353.

[23] P. Kaur, K. J. Singh, M. Kurudirek, and S. Thakur, 2019. Study of environment friendly bismuth incorporated lithium borate glass system for structural, gamma-ray and fast neutron shielding properties. *Spectrochimica Acta Part A: Molecular and Biomolecular Spectroscopy,* 223, 117309.